

Similarity Measure of Moment Vectors as Image Quality Measure

Kim-Han Thung and Raveendran Paramesran

Electrical Department

Faculty of Engineering

University of Malaya

50603, Kuala Lumpur, Malaysia

Email: henrythung@gmail.com, ravee@gmail.com

Abstract—This paper proposes a similarity measure of moments vectors as an image quality metric (IQM). The moment vectors can be obtained by arranging the Tchebichef moments of (8×8) image block (except DC component) in a row. The similarity measure between the two moment vectors from the reference and the test image blocks can then be used to quantify the local distortions of an image. Similar measure is also done on the DC component of the two image blocks. The local quality index is the weighted sum of the similarity measures of the dc and ac moment components. The final quality score is obtained by average the local quality indices from all the image blocks. The algorithm is tested on the LIVE dataset, and compared with other IQMs (e.g. PSNR, SSIM, Wee's metric). The results showed that the proposed metric performs comparable with other metrics especially for overall distortions by recoding a nonlinear correlation coefficient of 0.933.

I. INTRODUCTION

Image quality metric (IQM) is vital in the development of the image processing algorithm such as enhancement, deblurring, denoising, etc., as it can be used to evaluate the their performance in term of the quality of the processed image.

Quality of an image can be assessed either subjectively through human evaluation or objectively through computer calculation. As human beings are the ultimate users of most of the multimedia applications (which involve media of image), the subjective human evaluation is thus the most reliable quality assessment method. However, this method is impractical for online application (e.g. quality control system in video streaming) as it is too slow, inconvenient and expensive. Thus, the focus of the current research in IQM is on the objective metric which aims to predict the quality of the image as closely to the human subjectivity as possible. There are basically three categories of objective IQM: full-reference, reduced-reference and no-reference, according to the availability of the reference or ideal image, where the reference image is either fully, partially or not available to the IQM, respectively. In this paper, we discuss on the formulation of the full-reference IQM.

In the full-reference quality assessment (FRQA), quality scores of the test images (distorted) are obtained based on the comparison with the reference image which is assumed to be perfect in quality. The easiest way of quality assessment perhaps is by direct pixel comparison between the two images.

Mean squared error (MSE) (or its variant, peak signal-to-noise ratio (PSNR)), for example, is the most widely used FRQA metric, where it is calculated by taking the average of the square pixel differences between the two images. Other convenient mathematical models [1], [2] have been investigated as well to approximate image quality by calculate the errors between the two images. Such mathematic models include average difference, maximum difference, absolute error, Peak MSE, Laplacian MSE, Minkowski error, structural content, normalized cross-correlation, correlation quality, Czekanowski distance, etc. These metrics are simple, straight forward, and fast, but they are also widely criticized as well for not correlating well with perceived quality measurement [3], [4]. One of the possible reasons is that the *Human Vision System* (HVS) characteristics are not considered in their models.

Hence, plenty of work has been done by considering HVS in their models [5]–[7]. Majority of the early HVS-based metric are based on the error sensitivity approach, where it is assumed that the image quality degradation is directly related to the visibility of error signal (difference between the reference and the distorted signal). In this approach, the error signal is computed from the transformed domain (e.g. DCT, separable wavelet transform, vertex transform) of the images, and normalized according to their visibility, as determined by psychophysics of human perception such as contrast sensitivity function (CSF), luminance masking, contrast masking, etc. This approach was pioneered by Mannos and Sakrison [8], and extended by many other researchers ([9]–[14]).

Though this approach is nearly universal accepted, there are a number of limitations, as discussed in [15]. In brief, HVS is a complex and nonlinear system that is not fully understood, and thus most of the HVS-based models rely on a number of assumptions and generalizations. Modern IQMs avoid the difficulties in the modeling of the complex early HVS model by using the top-down approach in their models. In [15], [16], Wang *et al.* have proposed a new framework, the structural similarity approach, where it is assumed that HVS is highly adapted to the natural scenes information, which is highly structured. Thus, a measure of structural information change (between the reference and the distorted image) should provide a good approximation to perceived image distortion. They use correlation between the reference and the test image

as structural comparison measure. This correlation, combining with 2 other non-structural distortion measures, the luminance and contrast comparison measure, forming a SSIM index [17]. The experimental results using LIVE database [18] show that the mean SSIM metric correlate satisfactorily with the human subjectivity.

Recently, Wee *et al.* [19] have proposed to use correlation of orthogonal moments between the two images as image quality measure. Two discrete orthogonal moments (Tchebichef and Krawtchouk) are tested in [19] using a moment correlation index. In this metric, the moment correlation indices are applied to nine low order moment values for every 8×8 non-overlapping image block, and the final quality score is obtained by averaging all the moment correlation indices. The results show that the orthogonal moments perform competitively with others quality metric. In this paper, we use another similarity measure of moments to improve the performance of the metric.

The organization of this paper is as follow. Section I is the introduction which reviews the precursors to the study reported and briefly describe the nature of the research reported in this paper. Section II describes the formulation of the metric in comparison. Section III describes the computation of Tchebichef moments which are used in this study. Section IV describes the similarity measure of the previous metrics and proposed a similarity measure of moment vectors as quality measure. Section V shows the experimental result using LIVE database. We conclude our paper in section VI.

II. IMAGE QUALITY METRICS

In this section, we list down the equations of the quality metrics used in comparison in this paper. The first metric PSNR is a pixel-based metric, where the error is computed throughout every pixels of the image. The second and third metrics are the block-based metrics, where the similarity measure (local quality index) is computed for each block of the image and take average to get the final quality score.

A. PSNR

PSNR is calculated from the MSE using the equation below:

$$\text{MSE} = \frac{1}{M \times N} \sum_{x=1}^M \sum_{y=1}^N \left(I(x, y) - \tilde{I}(x, y) \right)^2 \quad (1)$$

$$\text{PSNR} = 20 \log_{10} \left(\frac{255}{\sqrt{\text{MSE}}} \right) \quad (2)$$

where $I(x, y)$ and $\tilde{I}(x, y)$ are the reference image and the test image with coordinate (x, y) and size $(M \times N)$ respectively and assuming maximum gray level of 255 for 8bits/pixel monotonic image.

B. SSIM

SSIM [15] is consisted of three component: The luminance similarity ($l(\mathbf{x}, \mathbf{y})$), contrast similarity ($c(\mathbf{x}, \mathbf{y})$) and structural

similarity ($s(\mathbf{x}, \mathbf{y})$).

$$\begin{aligned} \text{SSIM}(\mathbf{x}, \mathbf{y}) &= f(l(\mathbf{x}, \mathbf{y}) \cdot c(\mathbf{x}, \mathbf{y}) \cdot s(\mathbf{x}, \mathbf{y})) \\ &= \frac{(2\mu_x\mu_y + C_1)(2\sigma_{xy} + C_2)}{(\mu_x^2 + \mu_y^2 + C_1)(\sigma_x^2 + \sigma_y^2 + C_2)} \end{aligned} \quad (3)$$

where $\{\mu_x, \sigma_x\}$ and $\{\mu_y, \sigma_y\}$ denote the mean intensity and standard deviation set of image block \mathbf{x} and image block \mathbf{y} , respectively, while σ_{xy} denote their cross correlation. C_1 and C_2 are small constants value to avoid instability problem when the denominator is too close to zero.

C. Wee's moment correlation index

Wee's moment correlation index [19] is given as:

$$Q(\mathbf{x}, \mathbf{y}) = \frac{(2M_x M_y) + C_1}{(M_x^2 + M_y^2) + C_1}, \quad (4)$$

where M_x and M_y denote the moments for the image block \mathbf{x} and \mathbf{y} respectively. The parameter C_1 is a small constant to prevent singularity problem when both M_x and M_y are zero. The M_x and M_y consisted of nine moment values, including one DC component. Thus, this measure can be seen as the average of similarity measures of eight non-DC moment components and one DC component between the reference and the test images.

III. TCHEBICHEF MOMENTS

Tchebichef moments are calculated from a set of orthogonal moment functions which can be used to extract pattern features from two-dimensional images. The set of Tchebichef moments are based on discrete Tchebichef polynomials [20]. The n th-order N -point Tchebichef polynomial is defined as

$$t_n(x; N) = n! \sum_{k=0}^n (-1)^{n-k} \binom{N-1-k}{n-k} \binom{n+k}{n} \binom{x}{k} \quad (5)$$

The set of N Tchebichef polynomials $t_n(x; N)$ forms a complete and finite set of discrete basis functions and satisfies the orthogonality condition

$$\sum_{x=0}^{N-1} t_p(x; N) t_q(x; N) = \rho(n; N) \delta_{pq} \quad (6)$$

where δ_{pq} is the Kronecker delta function and

$$\rho(n; N) = (2n!) \binom{N+n}{2n+1} \quad (7)$$

The Tchebichef moments of order $(p + q)$ of an image with intensity function $f(x, y)$, $x \in 0, 1, \dots, M-1$, $y \in 0, 1, \dots, N-1$ is defined as :

$$T_{pq} = \sum_{x=0}^{M-1} \sum_{y=0}^{N-1} \tilde{t}_p(x; M) \tilde{t}_q(y; N) f(x, y), \quad (8)$$

where $\tilde{t}_p(x; M)$ and $\tilde{t}_q(y; N)$ are the normalized Tchebichef polynomials given by

$$\tilde{t}_p(x; M) = \frac{t_p(x; M)}{\sqrt{\rho(p; M)}}, \quad \tilde{t}_q(y; N) = \frac{t_q(y; N)}{\sqrt{\rho(q; N)}} \quad (9)$$

For the rest of the paper, we will use $\tilde{t}_n(x)$ to represent $\tilde{t}_n(x; N)$ if not otherwise specified. $\tilde{t}_n(x)$ is the orthonormal version of Tchebichef polynomials and it can be calculated using the recurrence relation below [21]:

$$\begin{aligned} \tilde{t}_n(x) &= \alpha_1(2x + 1 - N)\tilde{t}_{n-1}(x) + \alpha_2\tilde{t}_{n-2}(x), \\ n &= 2, 3, \dots, N-1; \quad x = 0, 1, \dots, N-1 \end{aligned} \quad (10)$$

where

$$\begin{aligned} \alpha_1 &= \frac{1}{n} \sqrt{\frac{4n^2 - 1}{N^2 - n^2}} \\ \alpha_2 &= \frac{1 - n}{n} \sqrt{\frac{2n + 1}{2n - 3}} \sqrt{\frac{N^2 - (n - 1)^2}{N^2 - n^2}} \end{aligned} \quad (11)$$

The initial conditions for the above recursion can be obtained from the following equations:

$$\begin{aligned} \tilde{t}_0(x) &= \frac{1}{\sqrt{N}}, \\ \tilde{t}_1(x) &= (2x + 1 - N) \sqrt{\frac{3}{N(N^2 - 1)}} \end{aligned} \quad (12)$$

In Matlab, it is easier to calculate Tchebichef moments (8) in matrix form. The set of Tchebichef moments of a square image $\mathbf{I} = \{f(x, y)\}_{x,y=0}^{N-1}$ up to order $(p + q)$ can be determined by

$$\mathbf{T} = \mathbf{P}\mathbf{I}\mathbf{Q}^T \quad (13)$$

where \mathbf{P} and \mathbf{Q} are transformation matrices which contain Tchebichef polynomials of orders up to p and q respectively,

$$\begin{aligned} \mathbf{P} &= \begin{pmatrix} \tilde{t}_0(0) & \dots & \tilde{t}_0(N-1) \\ \vdots & \ddots & \vdots \\ \tilde{t}_p(0) & \dots & \tilde{t}_p(N-1) \end{pmatrix}, \\ \mathbf{Q} &= \begin{pmatrix} \tilde{t}_0(0) & \dots & \tilde{t}_0(N-1) \\ \vdots & \ddots & \vdots \\ \tilde{t}_q(0) & \dots & \tilde{t}_q(N-1) \end{pmatrix} \end{aligned} \quad (14)$$

and $(.)^T$ denotes the transpose of the matrix. The complete set of the Tchebichef moments of image \mathbf{I} can be obtained by using (13) and substituting values $p = N - 1$ and $q = N - 1$ in (14).

IV. SIMILARITY MEASURES OF MOMENT VECTORS

The similarity measures used by SSIM index and Wee's moment correlation index share the same basic form:

$$S_1 = \frac{2ab}{a^2 + b^2}, \quad (15)$$

where S_1 denotes similarity measure, while a and b denote the features from the reference and the test images, which are luminance and contrast for SSIM index and moments for Wee's metric. Figure 1[a] shows the plot of S_1 using a series of a and b value. As can be seen from the figure, the value S_1 ranges from 0 to 1 for positive a and b and it has a lower resolution at the upper part of the plot, where the step change of S_1 is small. For moments, the value of a and b can be negative, and the value of S_1 can range from -1 to 1. In the

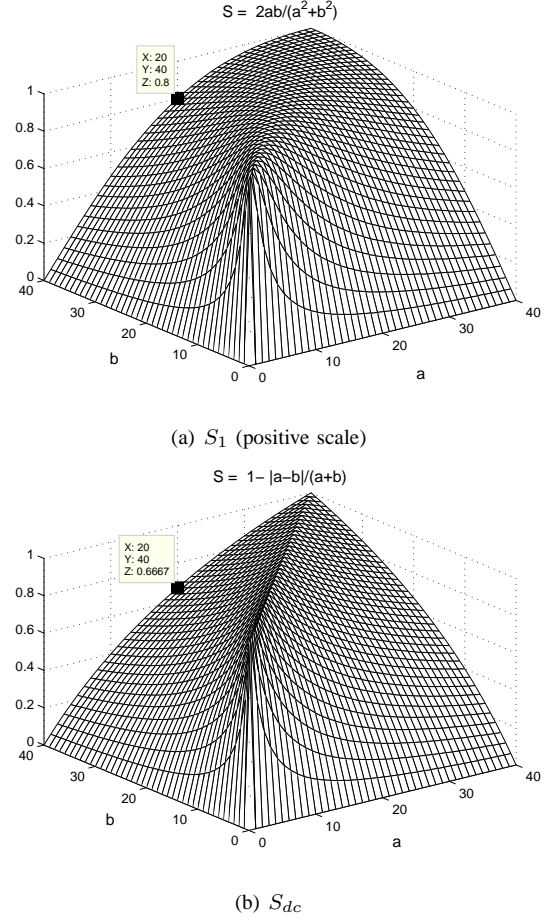


Fig. 1. Similarity Measures.

Wee's metric, 9 moments are calculated from each 8×8 block and the moment correlations are computed for each moments and averaged to obtain the final score. The possible weakness of the Wee's metric is listed follow:

- 1) For a small image block (8×8), there is a high possibility that only certain moment values are non-zero. The similarity measures of the zero moment values will cause singularity problem in equation 15. Though this singularity can be avoided by adding a small constant at the denominator and nominator (thus force the S_1 value to 1), this value is actually meaningless (similarity measure of nothing is 1?). However, in Wee's metric, these values are taken into account and averaged to get the final quality score.
- 2) The averaging method also ignores the different between the similarity measure of significant moment values (moment with high magnitude) and insignificant moment values (moment with small magnitude). Theoretically, the significant moments contain the main structural information of the image block and should be given higher weights than the less significant moments.

Thus, we have proposed another similarity measure to address this issue. Instead of compute the similarity measures

of moments between the two image blocks component by component, we compute the similarity measures of moment vectors between the two image blocks (8×8). The concept of the moment vector can be explained by first arrange the moments (except the DC component) from the image block A and B in a row:

$$\begin{aligned} \mathbf{a} &= [a_{01} \ a_{10} \ a_{11} \ \dots] \\ \mathbf{b} &= [b_{01} \ b_{10} \ b_{11} \ \dots] \end{aligned} \quad (16)$$

where a_{ij} and b_{ij} are the moments of order $(i + j)$ from the image block A and B respectively. We then call \mathbf{a} and \mathbf{b} as moment vectors. The similarity measure of moment vectors is defined as:

$$S_{ac} = 1 - \frac{|\mathbf{a} - \mathbf{b}|}{|\mathbf{a}| + |\mathbf{b}|} \quad (17)$$

This measure has the range of 0 to 1. Note that by using the concept of vector, and compare the vectors using the equation 17 above, the significant moments will mask out the less significant moments value automatically. Similarly, the similarity measure of the zero order moment (DC component) is defined as

$$S_{dc} = 1 - \frac{\text{abs}(a_{00} - b_{00})}{a_{00} + b_{00}} \quad (18)$$

The S_{dc} also range from 0 to 1, and to avoid the singularity problem, we add a small constant (0.001) to the denominator of the equation 18. The Figure 1[b] shows the plot of the S_{dc} . As shown in the figure, the S_{dc} has a more uniform resolution to detect the difference between a and b. The plot of S_{ac} is not shown here because it involves vectors (multiple subspaces), and thus can not be plotted directly using a 3D graph. The local quality index is then obtained by combines the similarity measure of moment vectors (ac part) and similarity measure of zero order moment (dc part) using the following equation:

$$S_{\text{local}} = w_{ac} \cdot S_{ac} + (1 - w_{ac}) \cdot S_{dc} \quad (19)$$

where the w_{ac} is the value from 0 to 1, denotes the weight between the S_{ac} and S_{dc} . When \mathbf{a} and \mathbf{b} are zero, there are no structural information, and thus w_{ac} is set to zero, making the local quality index a measure of only S_{dc} . In this way, we avoid adding dummy values to the metric when both the moment vectors \mathbf{a} and \mathbf{b} are zero, and also solve the singularity problem in equation 17. In other circumstances, the w_{ac} is set to a constant value. Five w_{ac} (0.2, 0.4, 0.5, 0.6 and 0.8) are tested in this study. The final quality score is obtained by averaging the local quality indices from all the image blocks:

$$Q = \text{mean}(\mathbf{S}_{\text{local}}) \quad (20)$$

where $\mathbf{S}_{\text{local}}$ is the matrix of local quality indices from all the image blocks of the image.

V. EXPERIMENTAL RESULTS

LIVE database [18] are used to evaluate the performance of the metric. This database consists of 29 original 24-bits/pixel color images and 779 distorted images representing five types

of distortions, including 175 JPEG compressed, 169 JPEG-2000 compressed, 145 Gaussian white noisy (GWN), 145 Gaussian blurred (GB) and 145 fast fading (FF) Rayleigh channel noisy images. In this paper, the new realigned DMOS quality scores [7] are used for the testing and analysis.

In this study, grayscale versions of the images were used for objective quality assessment by using pixel-wise transformation of $Y = 0.2989R + 0.5866G + 0.1145B$, where Y , R , G and B denote the 8-bit grayscale (luminance), red, green, and blue intensities of the images respectively. The objective scores predicted by the metric might not correlate linearly with the subjective scores, and thus a nonlinear regression is needed. The following logistic function with monotonic constraint was used for nonlinear fitting the objective quality scores with the subjective scores [15], [22]:

$$f(x) = \frac{\tau_1 - \tau_2}{1 + e^{\frac{x - \tau_3}{\tau_4}}} + \tau_2 \quad (21)$$

where the parameters τ_1 , τ_2 , τ_3 and τ_4 that minimized the sum of squared errors between the transformed metric output $\{f(x)\}$ and the corresponding subjective ratings are obtained by using Matlab *nlinfit* function.

Three performance metrics were chosen to evaluate the new proposed metric in this paper [23]: Pearson linear *correlation coefficient* (CC), the *root-mean-square error* (RMSE) (after nonlinear regression), which give us the measure of prediction accuracy and prediction error respectively. The third metric is the *Spearman rank-order correlation coefficient* (ROCC) which tells us the degree to which the model's predictions agree with the relative magnitudes of subjective quality ratings.

The Table I shows the performance of the metrics. As shown in the table, the proposed metric shows improvement of prediction for overall distortions when lower w_{ac} is used. Figure 2 shows the scatter plots between the DMOS and the output from the proposed metric when the parameter $w_{ac} = 0.2$ is used.

VI. CONCLUSION

In this paper, we used a new similarity measures to measure the moment correlation between the reference and the test images. The concept of moment vector is introduced in this new similarity measure. We also split the similarity measures into two parts, the dc part and the ac part. The local quality index is the weighted sum between the similarity measure of the ac and dc component of the block moments. The similarity of the ac component is discarded when there is no ac activity in the image block (both moment vectors are zero). Several weights between similarity measures of the ac component and the dc component are tested. The metrics are tested on the LIVE database, and the results show that the new similarity measure can improve the performance of the metric for overall distortions, especially when lower weight is used for the ac component. However, it is also noted that for individual distortion (especially the JPEG2000), the new similarity measure does not perform as satisfactory as the Wee's metric.

TABLE I
RESULTS BASED ON REALIGNED DMOS SCORES [7].

Measure	Metric	Distortion Type					
		JPEG-2000	JPEG	White Noise	Blurring	Fast Fading	All
Correlation Coefficient	PSNR	0.900	0.888	0.986	0.783	0.890	0.870
	SSIM	0.966	0.979	0.970	0.945	0.949	0.938
	Tch-wee [19]	0.959	0.943	0.973	0.952	0.954	0.919
	$Q(w_{ac}=0.2)$	0.926	0.945	0.957	0.963	0.954	0.933
	$Q(w_{ac}=0.4)$	0.906	0.934	0.945	0.961	0.957	0.925
	$Q(w_{ac}=0.5)$	0.900	0.930	0.940	0.960	0.957	0.921
	$Q(w_{ac}=0.6)$	0.896	0.928	0.934	0.959	0.957	0.919
	$Q(w_{ac}=0.8)$	0.890	0.925	0.924	0.958	0.956	0.914
RMSE	PSNR	11.018	14.656	4.702	11.480	13.016	13.471
	SSIM	6.483	6.515	6.788	6.052	9.005	9.449
	Tch-wee [19]	7.188	10.588	6.501	5.680	8.580	10.789
	$Q(w_{ac}=0.2)$	9.55	10.41	8.14	4.96	8.57	9.85
	$Q(w_{ac}=0.4)$	10.68	11.41	9.13	5.10	8.26	10.41
	$Q(w_{ac}=0.5)$	10.99	11.67	9.57	5.17	8.27	10.62
	$Q(w_{ac}=0.6)$	11.22	11.86	9.96	5.23	8.31	10.80
	$Q(w_{ac}=0.8)$	11.52	12.12	10.67	5.32	8.38	11.09
SROCC	PSNR	0.895	0.875	0.985	0.782	0.891	0.874
	SSIM	0.961	0.975	0.969	0.951	0.955	0.947
	Tch-wee [19]	0.953	0.938	0.954	0.959	0.958	0.918
	$Q(w_{ac}=0.2)$	0.919	0.938	0.943	0.960	0.951	0.925
	$Q(w_{ac}=0.4)$	0.899	0.930	0.922	0.955	0.950	0.915
	$Q(w_{ac}=0.5)$	0.893	0.929	0.914	0.954	0.950	0.912
	$Q(w_{ac}=0.6)$	0.888	0.927	0.910	0.953	0.949	0.910
	$Q(w_{ac}=0.8)$	0.882	0.924	0.899	0.951	0.948	0.906

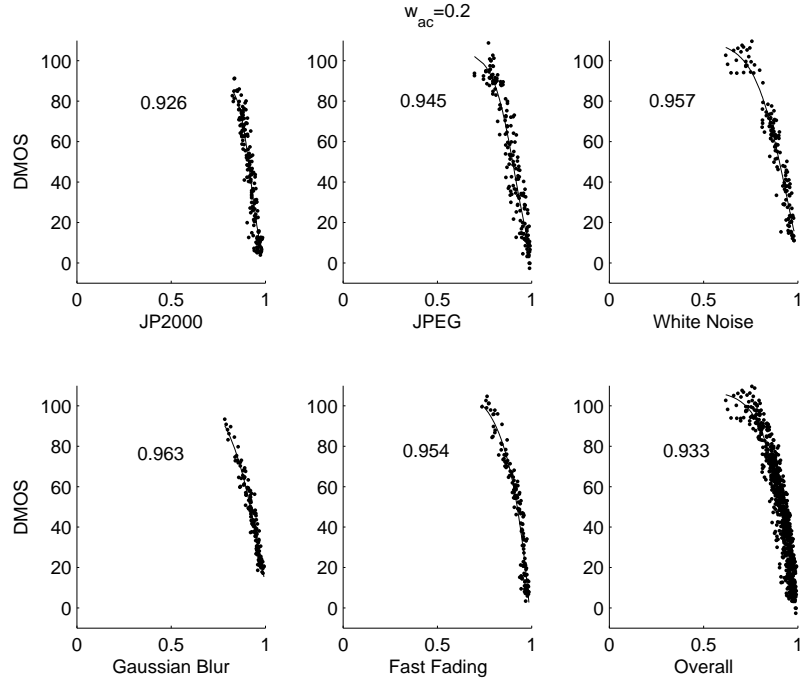


Fig. 2. Performance of the proposed metric when $w_{ac} = 0.2$.

ACKNOWLEDGMENT

The authors would like to thank anonymous reviewers for their valuable comments and suggestions to improve the quality of this paper.

REFERENCES

- [1] A. M. Eskicioglu and P. S. Fisher, "Image quality measures and their performance," *IEEE Trans. Commun.*, vol. 43, no. 12, pp. 2959–2965, 1995.
- [2] İsmail Avcıbaşı, "Image quality statistics and their use in steganalysis and compression," Ph.D. dissertation, Boğaziçi University, 2001.
- [3] B. Girod, "What's wrong with mean-squared error," in *Digital images and human vision*, A. B. Watson, Ed. Cambridge, MA, USA: MIT Press, 1993, ch. 15, pp. 207–220.
- [4] Z. Wang and A. Bovik, "Mean squared error: Love it or leave it? a new look at signal fidelity measures," *IEEE Signal Process. Mag.*, vol. 26, no. 1, pp. 98–117, 2009.
- [5] Z. Wang, H. R. Sheikh, and A. C. Bovik, "Objective video quality assessment," in *The Handbook of Video Databases: Design and Applications*, B. Furht and O. Marqure, Eds. Laboratory for Image and Video Engineering (LIVE), The University of Texas at Austin, Austin, TX 78712: CRC Press, Sept 2003, ch. 41, pp. 1041–1078.
- [6] İsmail Avcıbaşı, B. Sankur, and K. Sayood, "Statistical evaluation of image quality measures," *Journal of Electronic Imaging*, vol. 11, pp. 206–223, 2002.
- [7] H. R. Sheikh, M. F. Sabir, and A. C. Bovik, "A statistical evaluation of recent full reference image quality assessment algorithms," *IEEE Trans. Image Process.*, vol. 15, no. 11, pp. 3440–3451, Nov. 2006.
- [8] J. Mannos and D. Sakrison, "The effects of a visual fidelity criterion of the encoding of images," *IEEE Transactions on Information Theory*, vol. 20, no. 4, pp. 525–536, Jul 1974.
- [9] S. Daly, *Digital Image and Human Vision*. MIT Press, 1993, ch. The visible difference predictor: an algorithm for the assessment of image fidelity, pp. 179–206.
- [10] J. Lubin, *Digital Images and Human Vision*. MIT Press, 1993, ch. The use of psychophysical data and models in the analysis of display system performance, pp. 163–178.
- [11] A. B. Watson, "DCT quantization metrics visually optimized for individual images," in *Proc. SPIE*, ser. Human Vision, Visual Processing, and Digital Display IV, B. E. Rogowitz, Ed., vol. 1913, 1993, pp. 202–216.
- [12] P. C. Teo and D. J. Heeger, "Perceptual image distortion," in *ICIP-94*, vol. 2. ICI, 1994, pp. 982–986.
- [13] J. Lubin, *A visual discrimination model for imaging system design and evaluation*. World Science Publishing Co. Pte. Ltd., 1995, ch. 10, pp. 245–283.
- [14] T. N. Pappas and R. J. Safranek, "Perceptual criteria for image quality evaluation," in *Handbook of Image and Video Processing*. Academic Press, 2000, pp. 669–684.
- [15] Z. Wang, A. C. Bovik, H. R. Sheikh, and E. P. Simoncelli, "Image quality assessment: from error visibility to structural similarity," *IEEE Trans. Image Process.*, vol. 13, no. 4, pp. 600–612, 2004.
- [16] Z. Wang and A. Bovik, "A universal image quality index," *IEEE Signal Process. Lett.*, vol. 9, no. 3, pp. 81–84, Mar 2002.
- [17] Z. Wang, A. C. Bovik, and E. P. Simoncelli, "Structural approaches to image quality assessment," in *Handbook of Image and Video Processing*, A. Bovik, Ed. Laboratory for Computational Vision, New York University, New York, NY 10003; Laboratory for Image and Video Engineering (LIVE), The University of Texas at Austin, Austin, TX 78712: Academic Press, May 2005, ch. 8.3.
- [18] H. R. Sheikh, Z. Wang, L. Cormack, and A. C. Bovik, "Live image quality assessment database release 2." [Online]. Available: <http://live.ece.utexas.edu/research/quality>
- [19] C. Y. Wee, R. Paramesran, R. Mukundan, and X. Jiang, "Image quality assessment by discrete orthogonal moments," *Pattern Recognition*, vol. 43, no. 12, pp. 4055–4068, 2010. [Online]. Available: <http://www.sciencedirect.com/science/article/B6V14-506RMTW-2/2/d15009974247a8cf5514044cc75b92a7>
- [20] R. Mukundan, S. H. Ong, and P. A. Lee, "Image analysis by tchebichef moments," *IEEE Trans. Image Process.*, vol. 10, no. 9, pp. 1357–364, Sept 2001.
- [21] R. Mukundan, "Some computational aspects of discrete orthonormal moments," *IEEE Trans. Image Process.*, vol. 13, no. 8, pp. 1055–1059, Aug. 2004.
- [22] VQEG, "Final report from the video quality experts group on the validation of objective models of video quality assessment," <http://www.vqeg.org/>, Tech. Rep., 2000.
- [23] —, "Final report from the video quality experts group on the validation of objective models of video quality assessment, phase ii," <http://www.vqeg.org/>, Tech. Rep., 2003.